1. Title page

Title:

Human *in vivo* liver and tumor bioimpedance measured with biopsy needle

Authors:

Sanna Halonen (1,2), Ali Ovissi (3), Sonja Boyd (4), Juho Kari (1), Kai Kronström (1), Juhani Kosunen (3), Hanna Laurén (5), Kirsti Numminen (3), Harri Sievänen (1), Jari Hyttinen (2)

Affiliations:

(1) R&D Department, Injeq Oy, Biokatu 8, 33520 Tampere, Finland

(2) Faculty of Medicine and Health Technology, BioMediTech, Tampere University, Arvo Ylpön katu 34, 33520 Tampere, Finland

(3) Department of Radiology, Meilahti Hospital, Helsinki University Hospital, Haartmaninkatu 4, 00029 HUS, Helsinki, Finland

(4) HUS Diagnostic Center, Pathology, Helsinki University Hospital, PB 340, 00029 HUS, Helsinki, Finland

(5) Department of Radiology, Comprehensive Cancer Center, Helsinki University Hospital, Haartmaninkatu 4, 00029 HUS, Helsinki, Finland

Corresponding author:

Sanna Halonen, Biokatu 8, 33520 Tampere, Finland, sanna.halonen@injeq.com, tel. +358 50 4089171

Keywords

Bioimpedance, *in vivo*, liver biopsy, electrical impedance, clinical test, frequency spectrum, hepatic, tumor conductivity, needle guidance, tumor detection

2. Abstract

Objective: Liver biopsy is an essential procedure in cancer diagnostics but targeting the biopsy to the actual tumor tissue is challenging. Aim of this study was to evaluate the clinical feasibility of a novel bioimpedance biopsy needle system in liver biopsy and simultaneously to gather *in vivo* bioimpedance data from human liver and tumor tissues.

Approach: We measured human liver and tumor impedance data *in vivo* from 26 patients who underwent diagnostic ultrasound-guided liver biopsy. Our novel 18G core biopsy needle tip forms a bipolar electrode that was used to measure bioimpedance during the biopsy in real-time with frequencies from 1 kHz to 349 kHz. The needle tip location was determined by ultrasound. Also, the sampled tissue type was determined histologically.

Main results: The bioimpedance values showed substantial variation between individual cases, and liver and tumor data overlapped each other. However, Mann-Whitney U test showed that the median bioimpedance values of liver and tumor tissue are significantly ($p<0.05$) different concerning the impedance magnitude at frequencies below 25 kHz and the phase angle at frequencies below 3 kHz and above 30 kHz.

Significance: This study uniquely employed a real-time bioimpedance biopsy needle in clinical liver biopsies and reported the measured human *in vivo* liver and tumor impedance data. Impedance is always device-dependent and therefore not directly comparable to measurements with other devices. Although the variation in tumor types prevented coherent tumor identification, our study provides preliminary evidence that tumor tissue differs from liver tissue *in vivo,* and this association is frequency-dependent.

3. Introduction

Liver biopsies are essential for diagnostic purposes and treatment decisions concerning tumors and liver diseases. However, the biopsy procedure may be challenging, and it is often difficult to get a proper sample. According to Abdi et al (1979) only 46% of metastatic carcinoma were detected at the first liver biopsy, whereas in a more recent studies employing ultrasound guidance, malign lesions were identified by core-needle biopsy in 80.6% (Stewart et al 2002) and 93.5% (Vernuccio et al 2019) of the cases. In cancer diagnostics, it is highly important to collect a tissue sample from vital tumor tissue. If the sample does not contain tumor tissue or the sample is fully necrotic, histological diagnosis cannot be performed, and the patient needs to wait for another appointment for biopsy and a new analysis of the specimen. If a failure in tissue sampling is detected during the biopsy procedure, the operating radiologist could repeat the biopsy immediately. However, visual inspection of the biopsy specimen is often inadequate for assessing the sample quality. Thus, real-time identification of the correct biopsy spot would greatly benefit the procedure.

Imaging modalities are utilized in the liver biopsy to guide the procedure, but each method has its limitations (Shaw and Shamimi-Noori 2014). Ultrasound requires long-term training and may have an insufficient resolution. In ultrasound, highly reflecting objects, such as bones, cause shadowing effects to the image, and therefore tricky located liver tumors may remain hidden due to the blind spots caused by ribs. On the other hand, some soft tissue targets are rendered nonvisible and therefore tumor target may remain indistinguishable from surrounding liver tissue. Even if the target is well identified, localization of the needle and its tip can be challenging from the ultrasound frame due to difficulties in image plane alignment and imaging artifacts, such as reverberations, comet tails and shadowing effects (Chapman et al 2006). Also, computed tomography imaging may be utilized in the biopsy guidance, but at the price of a high radiation dose to the patient and personnel, and as the 3D tomography needs multiple projections, the method is not truly real-time.

Currently used imaging methods would benefit from innovations that would make the methods more accurate and/or easier to use. Bioimpedance measurement has been integrated into several medical instruments for target tissue detection and preliminary results from animal studies and *ex vivo* studies aiming to develop needle guidance have been reported by multiple groups (Halonen et al 2015, Halonen et al 2019, Kalvøy et al 2009, Park et al 2018, Trebbels et al 2012) or cancer detection (Baghbani et al 2018, Cheng et al 2020, Hong et al 2021, Lee et al 1999, Mishra et al 2013). The potential benefit of the bioimpedance needle method would be that it provides real-time information in a harmless way and can be combined with currently used ultrasound imaging. Since measuring bioimpedance at the needle tip provides information about electrical properties of tissue, the information is independent, originating from different physical phenomena than ultrasound and the scale of the information is highly localized. Therefore, the bioimpedance method has the potential to add clinically relevant new information to help the physician insert the biopsy needle to the correct spot. This method may also inform the physician about tissue interface

penetrations, tissue types and whether the biopsy needle tip has reached the correct spot for tissue sampling. However, so far only a few attempts utilizing bioimpedance measurement have progressed to the clinical phase (Halonen et al 2017 a, Halonen et al 2017, Sievänen et al 2021). Moreover, there are no clinical reports that a liver biopsy has been performed with a biopsy needle with bioimpedance measurement. In general, we lack information on the electric impedance of human liver tissue measured *in vivo*.

Healthy liver tissue is constructed of small, approximately hexagonal shaped units called lobules. Each lobule has portal triads at the vertices and a central vein in the middle. In humans, the scale of these terminal structural units is mainly within the sub-millimeter range (Teutsch 2005). Primary and metastatic tumors may destroy normal liver tissue or cause excess growth of connective tissue (desmoplasia). Hepatocellular carcinomas are highly vascularized, while metastases may be hyper- or hypovascular (Gaiani et al 2001).

Changes in the structure, extracellular fluid and fat content can alter the electrical properties of tissues, a fact that can be utilized in differentiating between different tissue types by bioimpedance spectroscopy (Halonen et al 2019, Kalvøy et al 2009). Bioimpedance describes how biological tissue resists the flow of electrical alternating current through it. Several studies have assessed tumor differentiation in the liver (Haemmerich et al 2003, Haemmerich et al 2009, Laufer et al 2010, Prakash et al 2015, Smith et al 1986, Wang et al 2014). Most of these studies report that liver tumors are more conductive than liver parenchyma, but the results are mainly based on *ex vivo* specimen and animal studies. *In vivo* measurements of electrical conductivity in the human liver are scarce. Only one study has measured electric conductivity in six patients using a bipolar probe on the liver surface within the gigahertz frequency range (O'Rourke et al 2007), but no such data within the kilohertz region is available, let alone data from the inside of the liver tissue. An interesting finding in the only *in vivo* study (O'Rourke et al 2007) is that both the conductivity and permittivity differed significantly between the normal and malignant liver tissues *ex vivo*, but not *in vivo*. They stated that the wideband dielectric properties *in vivo* are different from *ex vivo*. This statement calls for *in vivo* studies.

Here we measured *in vivo* bioimpedance from human liver and tumor tissues and assess the clinical feasibility of bioimpedance spectroscopy in biopsy guidance. We report clinical results from liver biopsies of 26 patients with liver tumor using our novel biopsy needle with integrated bioimpedance measurement. This device enables *in vivo* real-time recording of the spectral bioimpedance over the entire biopsy procedure, finally entering the liver and the target tumor tissue. The locations of the needle tip in the surrounding liver and tumor tissues were determined by experienced physicians using ultrasound guidance. The biopsy samples were histologically analyzed, and the obtained precise tumor type permitted a comparison between the impedance values from different liver tissue types. Here we report the bioimpedance data from living liver and tumor tissues measured at the tip of the biopsy needle during actual clinical liver biopsy operations within the kilohertz range.

4. Materials and Methods

4.1 Patients

The present medical device investigation was conducted in Helsinki University Central Hospital, Medical Imaging Center, Radiology and Department of Oncology. A patient was eligible for the study if he/she gave an informed consent and was submitted to ultrasound-guided core liver biopsy for the diagnosis of a liver tumor or other abnormalities with identifiable non-tumorous liver tissue. A patient was excluded if he/she could not give the consent, was under-aged, pregnant, or contraindicated to liver biopsy.

This study comprised 26 patients, whose mean age was 69 (range 34-84) years. Eight patients (31%) were men.

Written informed consent was obtained from all 26 patients before the study. The study protocol was approved by the Ethics Committee of Helsinki University Hospital (372/13/03/02/2015), and the national competent authority (National Supervisory Authority of Health and Welfare (Valvira), Helsinki, Finland) was notified about the study before commencing it. The study was conducted following the Declaration of Helsinki and Good Clinical Practice. The study is registered in ClinicalTrials.gov (NCT02620228).

4.2 Biopsy procedure

Experienced physicians performed the ultrasound-guided core liver biopsies using an investigational biopsy device with bioimpedance measurement (Figure 1). The operating physician pressed the device button when the needle tip was at the target tissue (liver or tumor) and this way created the so-called timestamps to the recorded impedance data. First, when the tip of the biopsy needle reached the non-tumorous liver tissue, the physician marked the first timestamp, and when the needle was inside the tumor, the physician pressed the second timestamp. Any deviations, additional timestamps, or false timestamps were marked to the patient's case report form. The physician determined the needle location using ultrasound imaging (LOGIQ E9, GE Healthcare). The investigational device measured the impedance data and stored the data during the whole biopsy procedure, but this information was not used for determining the needle location. Duration of the procedures varied from 17 seconds to 179 seconds (mean 88 seconds) from the skin penetration to the biopsy sampling.

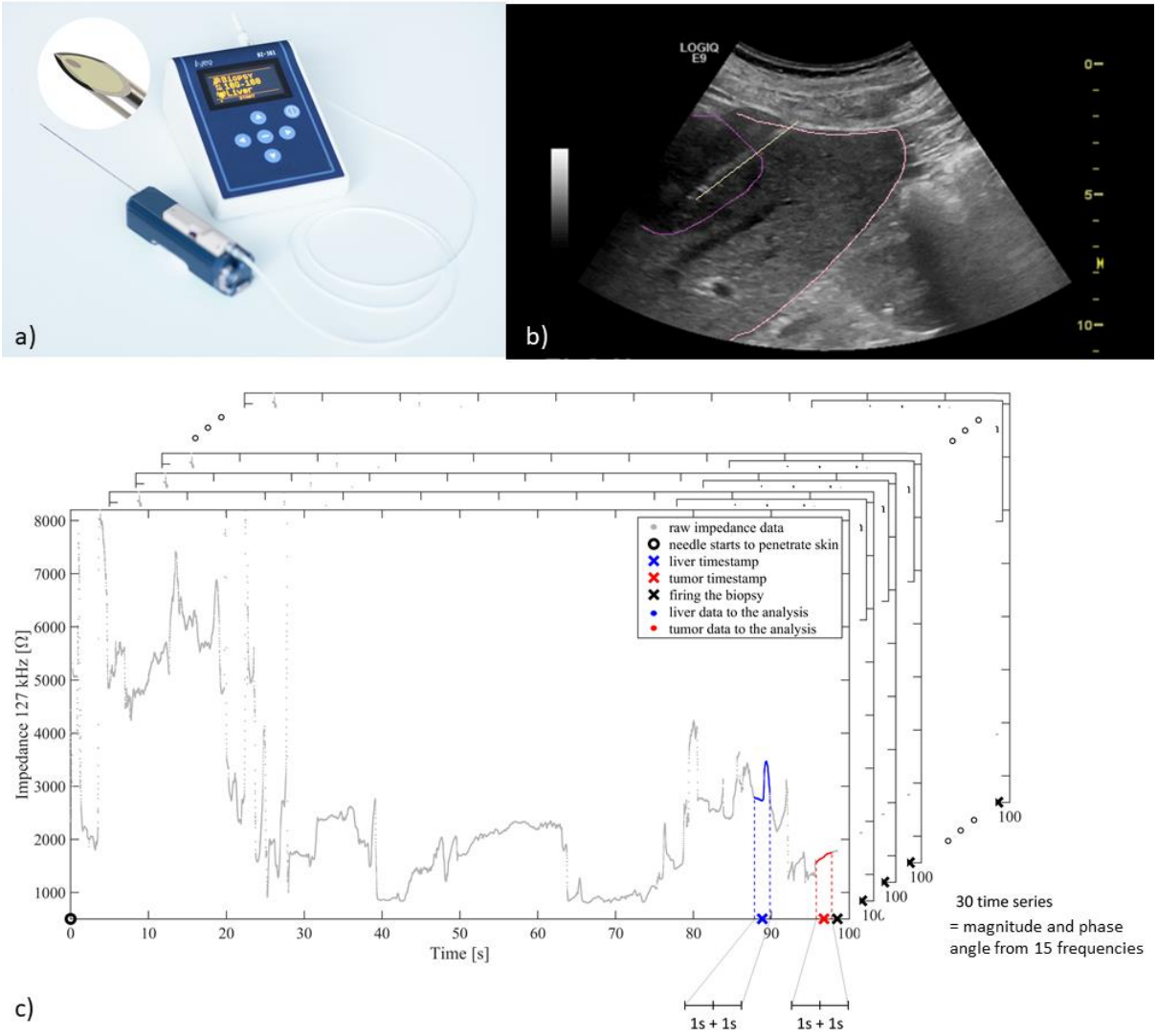

Figure 1. *The investigational device in the biopsy procedure. a) Biopsy needle and impedance analyzer (published previously in Halonen et al 2019 under the terms of the Creative Commons Attribution 4.0 International License (http://creativecommons.org/licenses/by/4.0/) and with kind permission of the copyright holder Injeq Oy). The needle is bipolar. The needle cannula is one electrode and the metal wire inside the needle is the other electrode. The inner electrode metal wire is insulated from the needle cannula with polymer insulator. The contact areas of the electrode are visible in the zoomed image of the needle tip. b) A still image from ultrasound video recorded during one biopsy procedure. The border of the liver (highlighted in pink), the biopsy needle (in yellow) and the border of the tumor (in violet) are shown. c) Impedance signal as a function of time during the entire biopsy procedure from skin penetration to the biopsy sampling. During the biopsy procedure, the physician marks the timestamp (blue and red crosses) when the needle tip is in the liver and tumor judged from the ultrasound image. Impedance data one second before and after the timestamps are utilized in the data analysis (blue and red). The black cross indicates the instant of firing the biopsy. Fifteen different frequencies are analyzed in real-time, which results in a total of 30 time series vectors (magnitude and phase angle).*

Whenever possible, the needle locations were ensured afterwards by analyzing the recorded ultrasound video by a physician who was not aware of the impedance data. However, the recorded video was available for the off-line reanalysis only in nine cases, although ultrasound imaging was utilized in all procedures.

Tissue samples were sent to the pathologist who analyzed them after standard tissue processing methods. The analysis was based on slides stained with hematoxylin-eosin. Ancillary tests were performed as needed. The following information was collected: sample size, amount of tumor, tumor type, and percentage of necrosis. If there was nonneoplastic liver tissue in the sample, the amount of fibrosis and steatosis was recorded. The pathologist was blinded to the impedance data. Histological analysis of biopsy samples was considered the final validation of whether the needle tip had been in the tumor or not.

Based on the histological assessment, liver parenchyma surrounding the tumor was normal in 13 patients, fibrotic in two, cirrhotic in one, steatotic in four, and not determined in six cases because biopsy did not include nonneoplastic liver. Examples of histology images and variation in the tissue types are shown in Figure 2. One can notice that, compared to normal liver parenchyma (Figures 2a and 2b), tumor tissues (Figures 2c-f) can be highly heterogenic including tumor cells, fibrosis, necrosis, or inflammation.

Twelve patients had adenocarcinoma (cholangiocarcinoma or adenocarcinoma metastasis from colorectal, lung, gynecological serous, breast, or of indefinite origin). Two patients had other metastatic carcinoma (renal carcinoma or indefinite origin), two had melanoma metastasis, and one had neuroendocrine tumor metastasis. Three patients had benign or premalignant hepatic lesion (hepatic adenoma, focal nodular hyperplasia, or dysplastic nodule) and two had hepatocellular carcinoma. Four samples were non-diagnostic (sample did not contain tumor, or tumor tissue was totally necrotic).

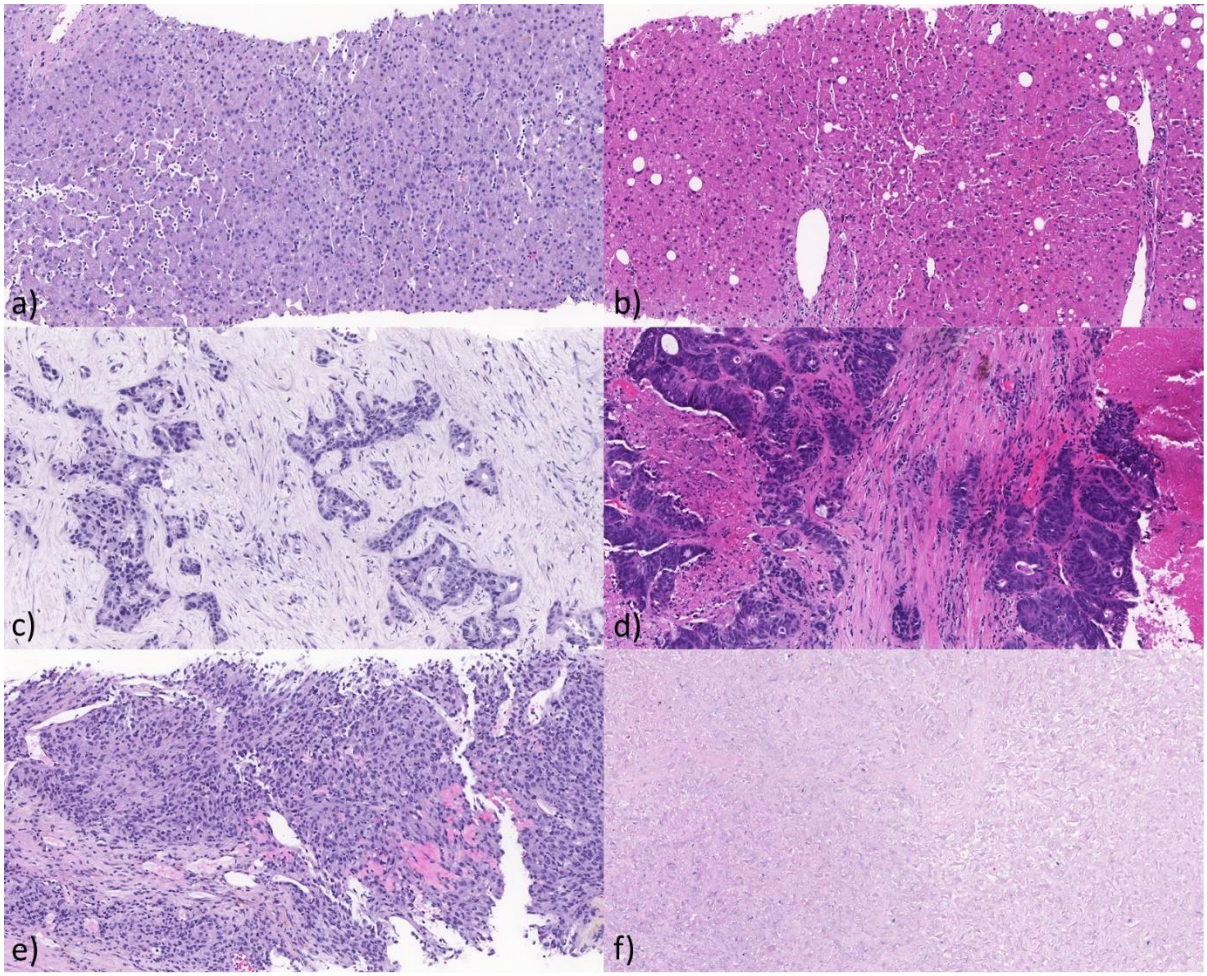

Figure 2. *Examples of human liver tissue histological samples, original magnification 200x, zoomed to the representative part having size of 1.08 mm x 0.58 mm. a) non-tumorous liver (some inflammation in sinusoids), b) non-tumorous liver with mild steatosis, c) adenocarcinoma (cholangiocarcinoma), d) adenocarcinoma (colorectal carcinoma metastasis), e) metastatic melanoma, and f) necrotic sample*

4.3 Investigational device

The investigational device (Figure 1) comprised a bioimpedance biopsy needle (IQ-Biopsy, Injeq Oy, Tampere Finland) that was connected to a real-time spectral impedance analyzer (Injeq BZ-301 analyzer, Injeq Oy, Tampere Finland). The biopsy needle is a customized core type biopsy needle that enables bioimpedance measurement from the tip of the needle using a bipolar measurement principle. The needle cannula is one electrode and the metal wire inside the needle is the other electrode. The inner electrode metal wire is insulated from the needle cannula with polymer insulator. The contact areas of the electrode are visible in the zoomed image of the needle tip in Figure 1a and schematic electric field in Figure 3. The needle size is 18G (outer diameter 1.27 mm). Sensitivity distribution of the impedance measurement is described elsewhere (Halonen et al 2019). Most of the measurement

sensitivity distribution is within volume 1 mm^3 from the needle tip facet (Halonen et al 2019). When the instrument trigger is pulled and the biopsy sample is collected, the impedance measurement stops. The impedance analyzer uses a 1 ms long binary pulse signal as an excitation signal. The pulse composition is designed in such a way that most of its power spectrum is at 15 specific frequency components from 1 kHz to 349 kHz. The excitation signal is continuously transmitted through the measurement circuit to the tissue, the transited signal measured and then the impedance at the specified frequencies calculated using Fourier transformation. The process is performed at the rate of 200 Hz. The device and measurement principle are described in more detail elsewhere (Halonen et al 2015, Halonen et al 2017b, Halonen et al 2019).

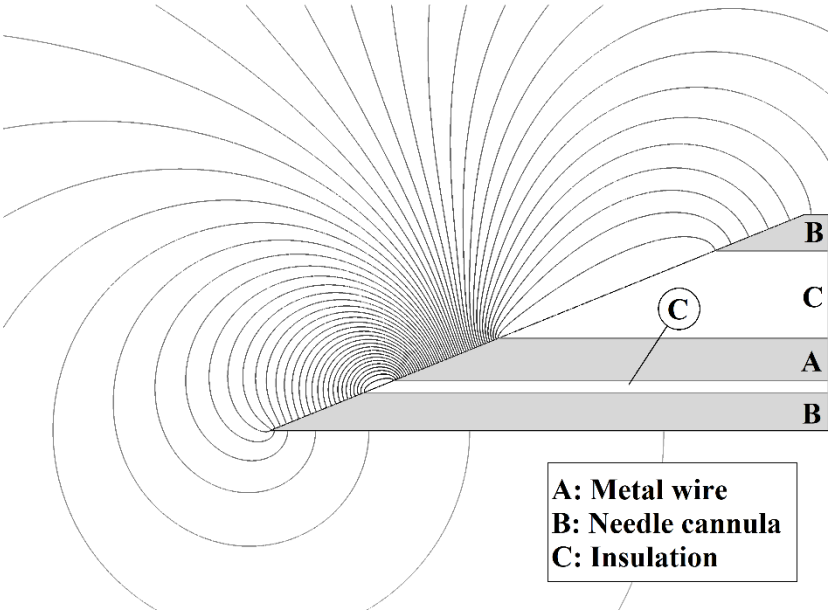

Figure 3. *Schematic electric field at the needle tip*

The needle tip electrode system measures the bioimpedance in a very small tissue volume (about one mm^3) and further the measured volume depends on the surrounding conductivity (Halonen et al 2019). Therefore, the estimation of the absolute tissue electric conductivity and permittivity becomes very complicated and vulnerable to errors. Further complicating matters, inherent features of bioimpedance measurement itself, include interface impedance and other interface phenomena especially at low measurement frequencies and capacitive coupling at high frequencies. Since this study focused on the differentiation between liver and tumor tissues, not on determining the absolute conductivity or permittivity values of these tissues, we primarily chose to present and compare directly the measured tissue impedance values.

Reproducibility of the device was evaluated by measuring the impedance of aqueous 0.3% and 0.9% saline solutions at room temperature with 11 different biopsy needles. Standard deviation (SD) of these 11 measurements was used as an index of reproducibility. We considered the 6% reproducibility acceptable to differentiate between tissues. When using only a single frequency impedance value, to be 95% confident that the measured impedance difference is actual, the observed difference between the two values should be greater than 2√2 times the reproducibility. The 6% reproducibility provides 95% confidence that a 17% difference in the measured impedance indicates an actual difference.

4.4 Data analysis

The overview of data accumulation is shown in Figure 4. Descriptive data of liver and tumor impedance data were based on the timestamps the operating physicians marked during the procedure. Data analysis was based on one second data periods before and after the timestamps (200+200 data points of spectral impedance data vectors) when the physician had judged that the needle tip location was in the correct spot of non-tumorous liver or tumor tissue (see Figure 1c). The needle moves during these two seconds within the target tissue structures, capturing the inherent variation in the impedance data due to tissue structures, as is the case in real clinical use. Thus, the raw data represent more than one single tissue spot of the target tissue.

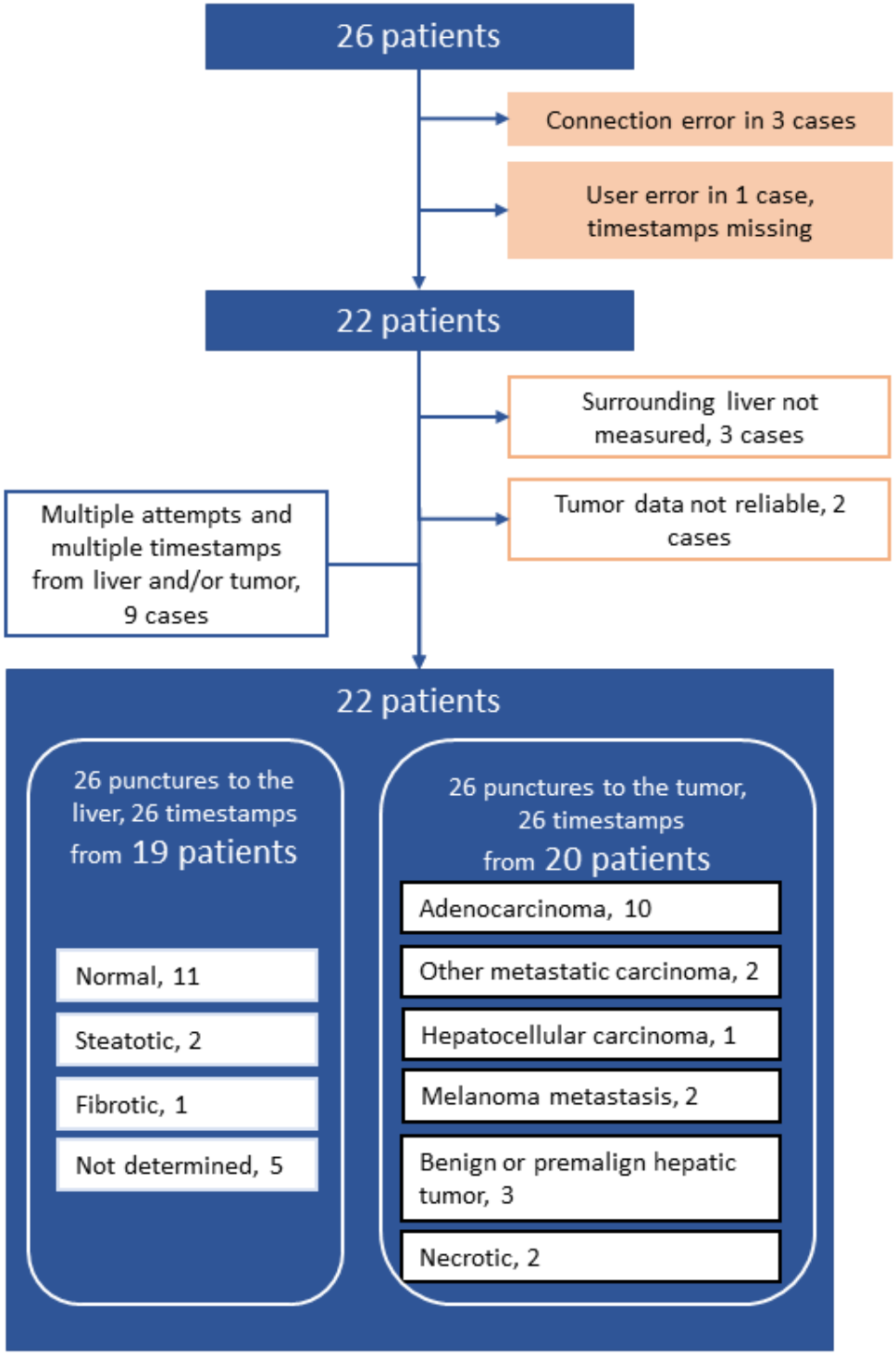

Figure 4. *Overview of included and excluded cases and timestamps.*

When there were multiple biopsy attempts, we included all data related to the timestamps in the analysis because the needle penetration route differed between attempts and

represented thus different tissue spots. In nine patients, the physician marked more than one timestamp in the liver and/or tumor tissue. All these timestamps were included in the analysis unless there was another reason to omit them. If the timestamp was marked after firing the biopsy or right at the time of the firing, the timestamp was relocated one second before the firing to obtain the same amount of data from these timestamps. In four patients, the timestamps were adjusted by 0.5-4 seconds based on the ultrasound video analysis by a physician who was unaware of the impedance information.

Raw data from 26 liver timestamps (26 x 200+200 spectral impedance data vectors) were pooled to the 'liver' group and from 26 tumor timestamps to the 'tumor' group. A 50% trimmed mean and quartiles were determined from the pooled raw data in these two groups and shown as frequency spectra. The 50% trimmed mean denotes the mean of data within the interquartile range (IQR), leaving out the highest 25% and the lowest 25% ends of the data and providing thus a noise-robust result. Frequencies 3 kHz and 127 kHz representing low and high measurement frequencies are described in more detail as histograms and tabulated data.

Subgroups of liver parenchymal types and tumor types were based on the pathologist's analysis of the biopsy specimen. A few of the biopsies were partly necrotic, but the subgroup 'necrotic' comprised the fully necrotic sample only. The impedances of different tumor types are reported as descriptive data without statistical comparison because of a small number of data in each subgroup.

The statistical comparison was done only between the 'liver' and 'tumor' groups. For statistical comparison, we calculated the 50% trimmed mean values for each timestamp at each measurement frequency. For the sake of clarity, we call these values puncture-wise trimmed means to discriminate them from the trimmed mean of raw data. Statistical comparison was based on the Mann-Whitney U test using the ranksum function in Matlab. This test was performed for all measurement frequencies and all puncture-wise trimmed means. A p-value < 0.05 was considered statistically significant.

5. Results

5.1. Reproducibility

Frequency spectra of saline solutions used in the reproducibility assessment are illustrated in Figure 5. As an index of reproducibility, standard deviation (SD) of these impedance magnitude measurements for 0.3% solution was less than 6% within the frequency range from 7 kHz up to the maximum of 349 kHz. For the solution 0.9%, the SD was 6% in 23-177 kHz. At the lower frequencies, SD increased to about 10%. The effect of electrode interface on the impedance was evident at the lower frequencies, but it declined rapidly, and the impedance magnitude become relatively constant at frequencies higher than 10 kHz.

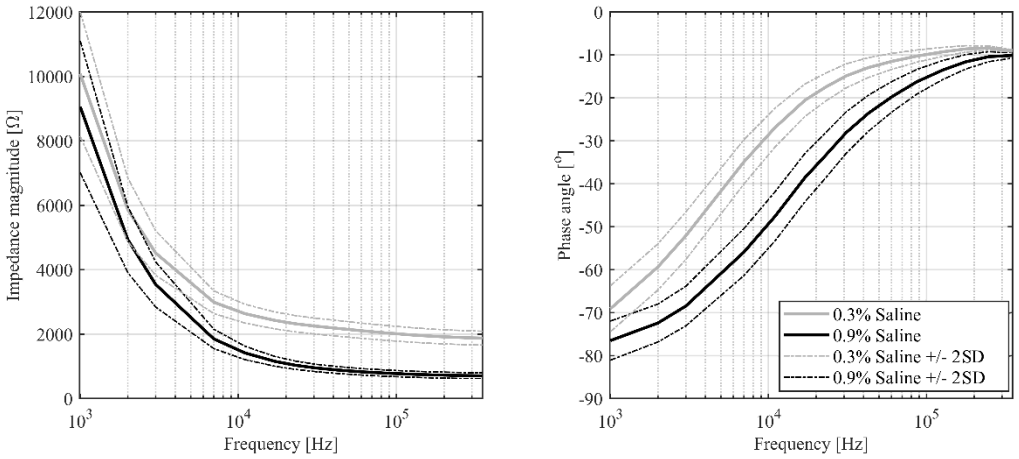

Figure 5. *Impedance magnitude (left panel) and phase angle (right panel) of 0.3% and 0.9% saline solutions against frequency.*

5.2 Human *in vivo* impedance data of liver and tumor

Impedance magnitude and phase angle spectra of the liver parenchyma and liver tumor tissue are presented in Figure 6. The values are calculated from the raw impedance data. The liver tissue shows a higher mean impedance magnitude through the measured frequency range, but the mean value remains within the quartile range of tumor data. Also, the phase angle data is partly overlapping between the liver and tumor tissues, but at the high end of frequencies, both the liver and tumor mean values are outside the quartiles of the other type of tissue. At 17 kHz, the phase angle spectra of liver and tumor intersect. At the lower frequencies, the liver tissue shows less negative phase angle than the tumor, while at the high frequencies it is the opposite.

Data distributions at 3 kHz and 127 kHz frequencies are shown and summarized in Figure 7. Tumor data representing multiple different tumor classes are more scattered compared to the liver data: interquartile ranges of tumor data are about two times wider.

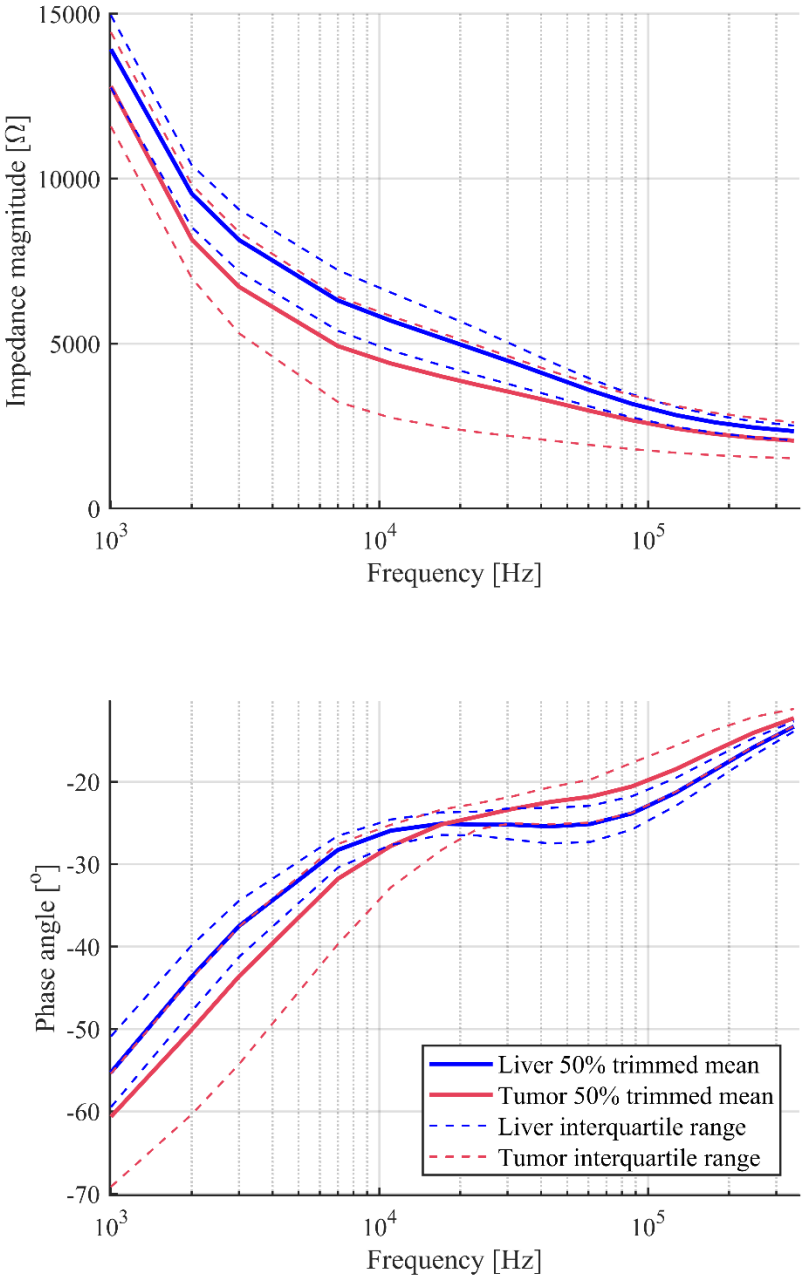

Figure 6. *Human in vivo liver and liver tumor impedance spectra. Impedance spectra mean of 50% data and interquartile ranges are calculated using raw impedance data collected around the liver and tumor timestamps (see Fig 1. for the definition of timestamp).*

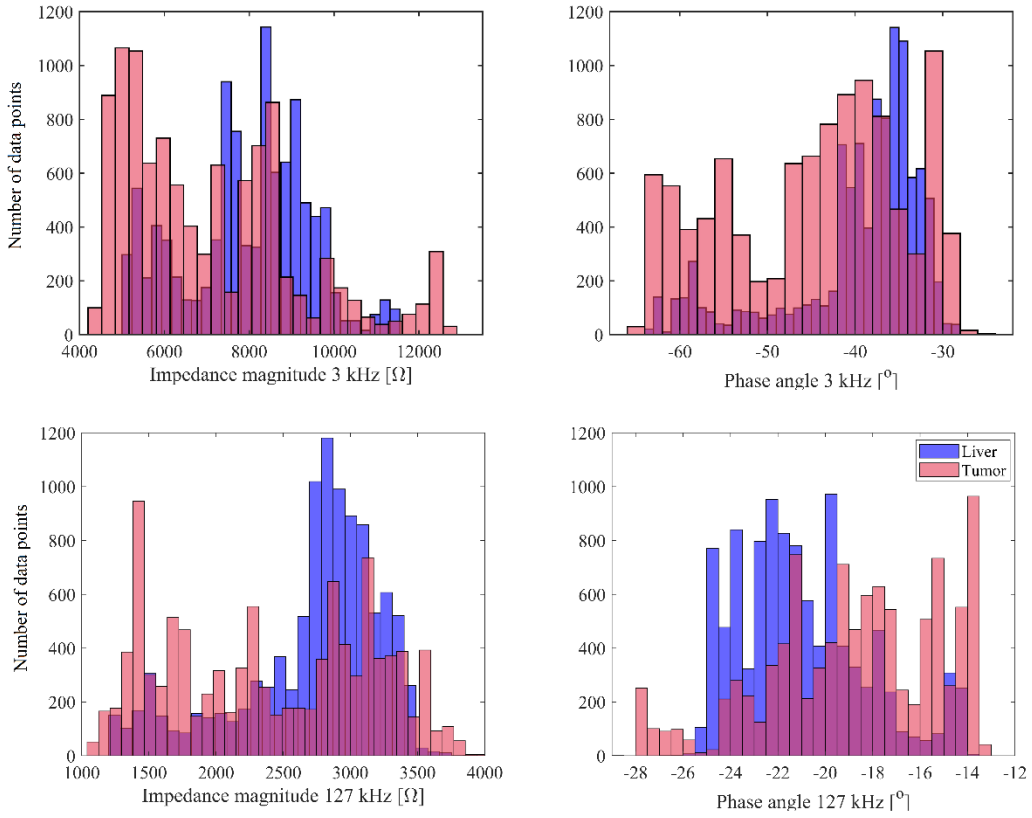

Figure 7. *Histograms of human in vivo liver (in blue) and liver tumor (in red) tissue raw impedance data at 127 kHz and 3 kHz around the timestamps. Note the overlap of histograms: red histogram overlapping the blue histogram looks pink. At 3 kHz, the trimmed mean impedance of liver tissue was 8143 Ω (IQR 7189 Ω – 9066 Ω) and that of tumor tissue 6724 Ω (IQR 5313 Ω – 8380 Ω). The respective phase angles were --38°* (IQR -41° – -34°) *and -44°* (IQR -54° – -38°). *At 127 kHz, the trimmed mean impedance of liver tissue was 2832 Ω (IQR 2477 – 3079) and that of tumor tissue 2426 Ω (IQR 1690 – 3110). The respective phase angles were --21°* (IQR -23° – -20°) *and -18°* (IQR -21° – -16°).

5.3 Human *in vivo* impedance of different liver and tumor types

Figure 8 illustrates the human *in vivo* raw impedance data in the liver, tumor, and histology-based subgroups. Most of the tissue subgroups overlap each other. Subgroups with one or two cases (steatotic, hepatocellular carcinoma, necrotic) stand out from the other groups in impedance, but since the number of data is so small, results are nonconclusive. Adenocarcinoma is the largest tumor group having 10 cases and 13 punctures. However, this group comprises various adenocarcinomas, which can explain large interquartile ranges.

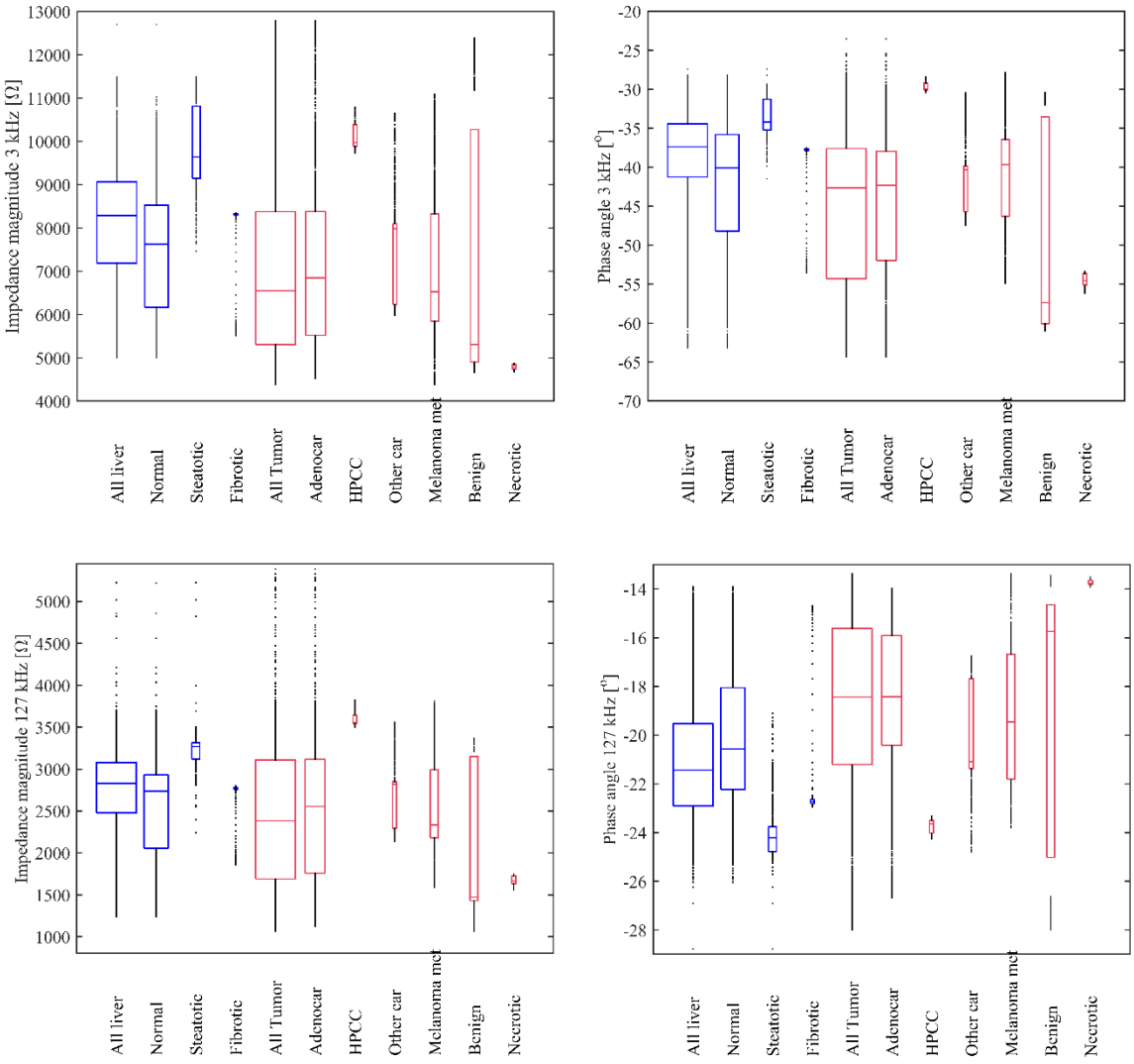

Figure 8. *Boxplots of impedance magnitude and phase angle in human in vivo liver (in blue) and liver tumor (in red) broken down by the tissue subgroup at 3 kHz and 127 kHz. Box shows the median and interquartile ranges of the raw impedance data around the timestamps (see details in Fig. 1). Box width is scaled based on the number of punctures (=timestamps) in the subgroup compared to the total number of liver/tumor punctures.*

5.4 Comparison of human *in vivo* liver and tumor tissue impedance

Primary statistical comparison was done between the puncture-wise trimmed means of the liver and tumor tissues at all 15 frequencies using the Mann-Whitney U test. Figure 9 illustrates the p-values of these differences as a function of frequency. Puncture-wise trimmed mean values around the timestamps are illustrated in Figure 10 for frequencies of 3 kHz and 127 kHz. According to the statistical comparison (Figure 9), liver and tumor tissues are significantly different from each other both in magnitude and phase angle in a frequency-specific manner. For the magnitude, significant differences (p-value <0.05) were observed at

low frequencies (< 25 kHz). For the phase angle, significant differences were observed both at the lowest frequencies (1 – 3 kHz) and the high frequencies (31 – 349 kHz). Whereas at the middle frequencies (10 – 25 kHz), close to the frequency the phase angle spectra crossed each other, the significance vanished rapidly.

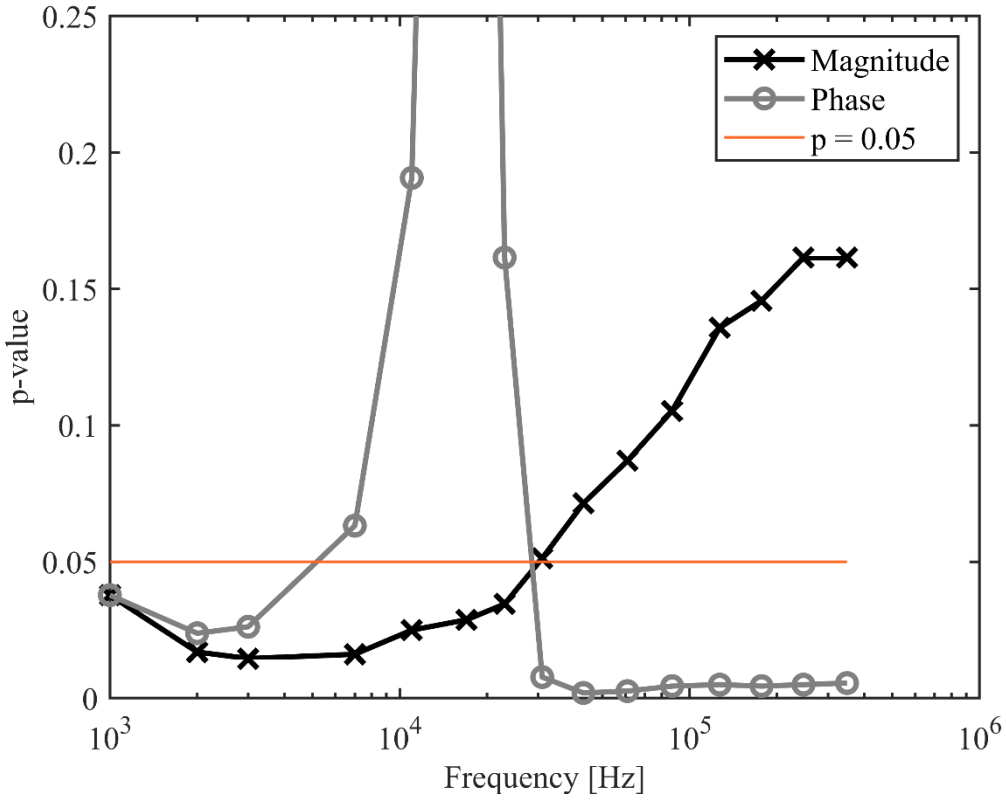

Figure 9. *The Mann-Whitney U test p-value as a function of measurement frequency from statistical comparisons between the human in vivo liver and liver tumor puncture-wise trimmed means of magnitude and phase angle data around the timestamps. Liver and tumor phase angle spectra intersect at 17 kHz and therefore the p-value has its peak (p=0.9).*

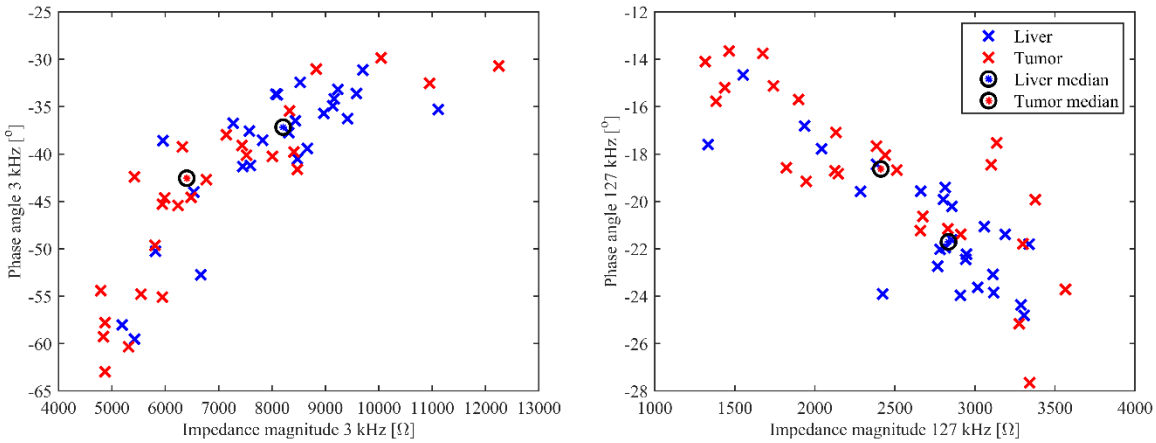

Figure 10. *Puncture-wise trimmed means of the human in vivo liver and tumor timestamp data at a single low (3 kHz) and high (127 kHz) frequency.* n_{Liver} *= 19,* n_{Tumor} *= 20.*

6. Discussion

The present study describes *in vivo* bioimpedance data of human liver tissues, including tumors, measured using bioimpedance spectroscopy within the kilohertz range during clinical biopsies of 26 patients. The collected clinical data provided a good basis to evaluate the feasibility of the bioimpedance needle in liver biopsy, providing realistic cases with varying tumor types and varying liver types. Most importantly, we showed that the liver and tumor tissues were different in terms of impedance magnitude and phase angle in a frequency-specific manner. We have previously shown that the needle-based impedance measurement for biopsy can achieve a good classification accuracy of different tissues in *in vivo* porcine model (Halonen et al 2019).

Impedance value in itself is always dependent on the measurement system and thus not necessarily comparable to measurements with other devices. However, the relative difference between impedance values (and conductivity values) from two tissues measured with same device is comparable to the measured relative differences with other devices. Whereas absolute impedance or conductivity values are not considered crucial for the application of tissue identification, reproducibly measured differences between tissue electrical properties are naturally required for the differentiation. The mean magnitude of impedance in the liver parenchyma was higher than in the tumor. This could be due to a higher conductivity in the liver tumor compared to the liver parenchyma. The difference in the impedance magnitude was significant at the frequencies below 30 kHz. However, our *in vivo* clinical data showed large variability, most likely due to heterogeneous liver pathologies, and thus there was substantial overlap between individual data. The higher conductivity seems to be a general property in tumors. Liver tumors (mainly metastasis) are reported to have even 5-7.5 times higher conductivities at 1 kHz than liver parenchyma in *ex vivo* animal and *ex vivo* human studies (Haemmerich et al 2009, Laufer et al 2010, Prakash et al 2015,

Smith et al 1986). At the higher frequencies, reported differences are smaller having 1.5-2 times higher conductivities at about 400 kHz (Haemmerich et al 2009, Laufer et al 2010, Prakash et al 2015). However, in these studies, the sample sizes were small including 4 to 10 cases. In a larger study of 116 cases (Wang et al 2014), *ex vivo* normal liver, hepatocellular carcinoma, hepatic fibrosis, and liver hemangioma were evaluated within a frequency range from 10 Hz to 100 MHz. These authors found that liver hemangioma had a higher conductivity compared to other liver tissues, but the other liver tissues did not differ significantly from each other. The fibrotic liver showed slightly higher permittivity and conductivity, and hepatocellular carcinoma slightly lower conductivity and permittivity than the normal liver tissue. Liver metastatic tumors were not measured in their study.

In the only single *in vivo* study of liver tumors addressing the kHz region, (Haemmerich et al 2003) the electrical properties of tumor tissue differed less from the liver tissue than was observed in the above-described *ex vivo* studies (Haemmerich et al 2009, Laufer et al 2010, Prakash et al 2015, Smith et al 1986). In this experimental study of rats, the authors injected colon cancer cells into the liver to initiate tumor growth, and they obtained data from a single type of tumor, grown in an otherwise healthy liver. Compared to the liver tissue, metastatic colon cancer in the liver was associated with about twice conductivity at 1 kHz and about 1.5 times higher at 100 kHz (Haemmerich et al 2003). In our study, the mean magnitude of liver impedance was about 1.2 times higher compared to the tumor at the frequencies of 3 kHz and 127 kHz. We conducted *in vivo* bioimpedance measurements from multiple tumor types that were detected in actual patients. The type, size, and stage of the tumors varied a lot, and these factors are known to affect the dielectric properties of tumors (Miklavčič et al 2006). In fact, the interquartile range (IQR) in the tumor data was about double compared to the liver data (Figure 7). Heterogeneity in the tumor group most likely explains the higher IQR in the impedance data compared to the IQR in the impedance of liver tissue. However, it is also possible that the tumors show more variation overall due to their unstructured cell and tissue architecture compared to the normal liver tissue. Overall, both in liver and tumor tissues, the percentage variation in the impedance data were distinctly higher than in the homogeneous saline solutions, thus most of this variation likely originates from the electrical and structural properties of the tissue.

In the literature, a higher conductivity of liver tumors is attributed to necrosis and the associated membrane breakdown (Haemmerich et al 2003). In our study, the lowest impedance indicating higher conductivity was measured from the fully necrotic sample.

In our study, the phase angle of tumor tissue was lower at frequencies below 17 kHz and less negative at higher frequencies compared to the phase angle of liver tissue. Suppose that the lower phase angle implies higher permittivity, our result suggests that the relative permittivity of the tumor is higher at the low frequencies than the permittivity of normal liver tissue, but the opposite at high frequencies. The difference in the phase angle was statistically significant at all frequencies except the middle frequencies where the liver and tumor phase angle curves intersected (7 – 23 kHz). Literature suggests a similar relationship, where the relative

permittivity of the liver tumor is 1.2 – 3 times higher at 1 kHz than that of the liver, whereas at 400 kHz, the normal liver had 1.1 – 1.4 times higher permittivity than the tumor (Laufer et al 2010, Prakash et al 2015).

Statistical comparison between the liver and tumor data revealed specific frequency-depended behavior for the magnitude and phase angle of impedance. Our findings indicate that at the measurement frequencies higher than 30 kHz, the phase angle provides a better differentiation than the magnitude. Within the frequency range 7 – 23 kHz, the magnitude provides a better differentiation, whereas at the lower frequencies both the magnitude and phase angle provide differentiation. The optimal frequency may depend on the measurement system and target tissue. In the literature comprising the *ex vivo* rabbit study (Smith et al 1986), experimental *in vivo* rat study (Haemmerich et al 2003), and *ex vivo* human study (Prakash et al 2015), liver tumors are best discriminated by employing the conductivity at frequencies below 100 kHz. Also, the *ex vivo* study of human samples found a significant difference in the permittivity between 100 Hz – 800 kHz, except between 8 – 20 kHz, (Prakash et al 2015) supporting our findings.

Although our material is by far the largest study measuring impedance during a human liver biopsy *in vivo*, the still relatively small sample size and especially the large variation in the tumor types limited our analysis. For example, in statistical analysis, all liver parenchymas and tumors were pooled and considered as two single groups. Since the different pathologies and non-malignant changes can alter the tissue bioimpedance differently, it would have been optimal to have a greater number of representative samples from each pathology. This would have required a much larger sample size.

It is well established that the temperature and electrolyte concentrations have a substantial impact on electrical conductivity of tissues. Exact temperatures or electrolyte concentrations of the patients were not monitored in our study, but the data was obtained from living patients, and it was assumed that temperature and electrolyte concentration variations were within the normal range. However, these factors can cause part of the variation in the impedance data.

Blood and body fluids constitute intrinsic components of tissue and therefore also intrinsic determinants of the impedance in an *in vivo* measurement. However, if the needle remains steady in the tissue for a long time, blood or body fluids may accumulate to the needle tip and decrease incorrectly the impedance value. In our study, measurements were primarily taken with a moving needle, which minimizes this concern. However, the needle speed was not monitored, and sporadic stops were likely to occur during the procedure, especially if the tumor was small and located deep in the liver.

The needle measures mostly the volume within 1 mm^3 from the needle tip (Halonen et al 2009). This causes spatiotemporal variation to the impedance values when the needle moves through various macro- and microscopic tissue structures. The biopsy sample, in turn, is about 2 cm long and taken ahead of the biopsy needle tip. Basically, the entire tissue volume where

the impedance measurement was done at the firing was also gathered to the biopsy sample, but the sampled tissue may also include tissue types that are outside the measured volume at the needle tip. Ultrasound-based timestamps were marked to the data to indicate the locations of liver parenchyma and liver tumor. This impedance data around the timestamps were used in the analysis, but the types of liver and tumor tissues were determined based on the pathologist's histological analysis of the entire biopsy specimen.

The precision of the timestamps depends not only on the precision of the operating physician but also on the visibility of the liver-tumor interface and the needle tip in the ultrasound image. All operating physicians were experienced and highly qualified to perform the liver biopsy operation, but overall, the procedure is challenging. Ultrasound imaging is a clinical routine that enabled real-time monitoring of the needle location and proper use of the investigational biopsy device without extra disturbances or changes to the clinical procedure. However, the uncertainty in ultrasound imaging is quite high when the millimeter-scale information on the needle tip location is required. The uncertainty in the exact needle tip location is one weakness of this study, but at the same time, it also emphasizes the need and utility of feasible guidance systems for biopsy procedures.

7. Conclusion

Bioimpedance offers a potential method for biopsy guidance by providing spatially precise real-time information on the tissue characteristics from the tip of the biopsy needle. However, while the present study indicates clinical feasibility for bioimpedance spectroscopy in transcutaneous liver biopsy, both the validation of clinical benefits and the development of proper tissue classification would require much larger patient materials representing sufficient numbers of patients with different types of tumors. The present device produces impedance data which - as is the case in all devices and electrode setups - depend on the characteristic configuration of the measuring electrode, i.e., the needle. Therefore, the present impedance results cannot be directly compared to data obtained by other devices. Our study is the first that measured *in vivo* the human liver and liver tumor tissue with bioimpedance spectroscopy in real-time during actual biopsy procedures. This independent information based on bioimpedance could essentially complement the information obtained from ultrasound imaging, which represents more large-scale information by nature and arises from different physical phenomena.

8. Acknowledgements

Conflict of interest

SH, JKa and HS are employees of Injeq Oy. SH, JKa, KK, JH and HS are shareholders of Injeq Oy. SH, JKa, KK are inventors of IQ-Biopsy related patents EP3484373 and EP3302290 owned by

Injeq Oy. KK and JH are co-founders of Injeq Oy. JH is a board member of Injeq Oy. SB, JKo, HL, KN, AO have nothing to declare.

9. References

Abdi W, Millan J C and Mezey E (1979). Sampling variability on percutaneous liver biopsy. *Archives of Internal Medicine* **139**(6) 667-669.

Baghbani R, Moradi M H and Shadmehr M B (2018). The development of a four-electrode bio-impedance sensor for identification and localization of deep pulmonary nodules. *Ann. Biomed. Eng*. **46**(8) 1079-1090.

Chapman G A, Johnson D and Bodenham A R (2006). Visualisation of needle position using ultrasonography. *Anaesthesia* **61**(2) 148-158.

Cheng Z, Carobbio A L C, Soggiu L, Migliorini M, Guastini L, Mora F, Fragale M, Ascoli A, Africano S, Caldwell D G *et al* (2020). SmartProbe: a bioimpedance sensing system for head and neck cancer tissue detection. *Physiol. Meas*. **41**(5) 054003.

Gaiani S, Volpe L, Piscaglia F and Bolondi L (2001). Vascularity of liver tumours and recent advances in Doppler ultrasound. *J. Hepatology* **34** 474-482.

Haemmerich D, Staelin S T, Tsai J Z, Tungjitkusolmun S, Mahvi D M and Webster J G (2003). In vivo electrical conductivity of hepatic tumours. *Physiol. Meas.* **24**(2) 251-260.

Haemmerich D, Schutt D J, Wright A W, Webster J G and Mahvi D M (2009). Electrical conductivity measurement of excised human metastatic liver tumours before and after thermal ablation. *Physiol. Meas.* **30**(5) 459–66.

Halonen S, Kari J, Ahonen P, Elomaa T, Annus P and Kronstrom K (2015). Biopsy needle including bioimpedance probe with optimized sensitivity distribution. *Int. J. Bioelectromagn* **17**(1) 26–30.

Halonen S, Kankaanpää E, Kari J, Parmanne P, Relas H, Kronström K, Luosujärvi R and Peltomaa R (2017a). Synovial fluid detection in intra-articular injections using a bioimpedance probe (BIP) needle—a clinical study. *Clin. Rheumatol.* **36**(6) 1349–1355.

Halonen S, Annala K, Kari J, Jokinen S, Lumme A, Kronström K and Yli-Hankala A. (2017b) Detection of spine structures with Bioimpedance Probe (BIP) Needle in clinical lumbar punctures. *J. Clin. Monit. Comput.* **31**(5) 1065–1072.

Halonen S, Kari J, Ahonen P, Kronström K and Hyttinen J (2019). Real-time bioimpedance-based biopsy needle can identify tissue type with high spatial accuracy. *Ann. Biomed. Eng.* **47**(3) 836-851.

Hong Y T, Yun J, Lee J H and Hong K-H (2021). Smart needle to diagnose metastatic lymph node using electrical impedance spectroscopy. *Auris Nasus Larynx* **48**(2) 281-287.

Kalvøy H, Frich L, Grimnes S, Martinsen Ø G, Hol P K and Stubhaug A (2009). Impedance-based tissue discrimination for needle guidance. *Physiol. Meas.* **30**(2) 129-140.

Laufer S, Ivorra A, Reuter V E, Rubinsky B and Solomon S B (2010). Electrical impedance characterization of normal and cancerous human hepatic tissue. *Physiol. Meas.* **31**(7) 995-1009.

Lee B R, Roberts W W, Smith D G, Ko H W, Epstein J I, Lecksell K and Partin A W (1999). Bioimpedance: novel use of a minimally invasive technique for cancer localization in the intact prostate. *Prostate* **39**(3) 213-218.

Miklavčič D, Pavšelj N and Hart F X (2006). Electric properties of tissues. *Wiley Encyclopedia of Biomedical Engineering*. John Wiley & Sons Inc.

Mishra V, Schned A R, Hartov A, Heaney J A, Seigne J and Halter R J (2013). Electrical property sensing biopsy needle for prostate cancer detection. *Prostate* **73**(15) 1603-1613.

O'Rourke A P, Lazebnik M, Bertram J M, Converse M C, Hagness S C, Webster J G and Mahvi D M (2007). Dielectric properties of human normal, malignant and cirrhotic liver tissue: in vivo and ex vivo measurements from 0.5 to 20 GHz using a precision open-ended coaxial probe. *Phys. Med. Biol.* **52**(15) 4707-4719.

Park J, Choi W M, Kim K, Jeong W I, Seo J B and Park I (2018). Biopsy needle integrated with electrical impedance sensing microelectrode array towards real-time needle guidance and tissue discrimination. *Sci. Rep.* **8**(1) 264.

Prakash S, Karnes M P, Sequin E K, West J D, Hitchcock C L, Nichols S D, Bloomston M, Abdel-Misih S R, Schmidt C R, Martin Jr E W *et al* (2015). Ex vivo electrical impedance measurements on excised hepatic tissue from human patients with metastatic colorectal cancer. *Physiol. Meas.* **36**(2) 315-328.

Shaw C and Shamimi-Noori S (2014). Ultrasound and CT-directed liver biopsy. *Clinical Liver Disease* **4**(5) 124–127.

Sievänen H, Kari J, Halonen S, Elomaa T, Tammela O, Soukka H and Eskola V (2021). Real-time detection of cerebrospinal fluid with bioimpedance needle in pediatric lumbar puncture. *Clin. Physiol. Funct. Imaging.* **41**(4) 303-309.

Smith S R, Foster K R and Wolf G L (1986). Dielectric properties of VX-2 carcinoma versus normal liver tissue. *IEEE Trans. Biomed. Eng.* **33**(5) 522-524.

Stewart C J R, Coldewey J and Stewart I S (2002) Comparison of fine needle aspiration cytology and needle core biopsy in the diagnosis of radiologically detected abdominal lesions. *J. Clin. Pathol.* **55**(2) 93-97.

Teutsch H F (2005). The modular microarchitecture of human liver. *Hepatology* **42**(2) 317-325.

Trebbels D, Fellhauer F, Jugl M, Haimerl G, Min M and Zengerle R (2012). Online tissue discrimination for transcutaneous needle guidance applications using broadband impedance spectroscopy. *IEEE Trans. Biomed. Eng.* **59**(2) 494-503.

Vernuccio F, Rosenberg M D, Meyer M, Choudhury K R, Nelson R C and Marin D (2019). Negative biopsy of focal hepatic lesions: decision tree model for patient management. *Am. J. Roentgenology* **212**(3) 677-685.

Wang H, He Y, Yang M, Yan Q, You F, Fu F, Wang T, Huo X, Dong X and Shi X (2014). Dielectric properties of human liver from 10Hz to 100MHz: normal liver, hepatocellular carcinoma, hepatic fibrosis and liver hemangioma. *Biomed. Mat. Eng.* **24**(6) 2725-2732.